Zdeněk Drozd[1], Zuzanka Trojanová[2], Aleš Jäger[3]
Charles University, Faculty of Mathematics and Physics, Ke Karlovu 3 (5), 121 16 Prague 2

MECHANICAL PROPERTIES OF QE22 MAGNESIUM ALLOY BASED COMPOSITES

Mechanical properties of two magnesium alloy based composites were studied. Composite with QE22 matrix reinforced by 20 vol.% of Al_2O_3 short fibres and hybrid composite (QE22 + 5 vol.% Al_2O_3 fibres and 15 vol.% SiC particles) were deformed in compression at temperatures from RT up to 400°C. Two types of specimens were investigated - one with fibres plane oriented parallel to the stress axis and the other with perpendicular fibres plane orientation. Temperature dependencies of the characteristic stresses σ_{02} and σ_{max} were studied. Mechanical properties of composite materials were compared with the monolithic QE22 matrix alloy. Optical and scanning electron microscopy were used for study of microstructure of materials. Possible hardening and softening mechanisms are discussed.

Key words: **composite, hybrid composite, hardening, softening**

WŁAŚCIWOŚCI MECHANICZNE KOMPOZYTÓW NA OSNOWIE STOPU MAGNEZU QE22

Przedstawiono wyniki badań właściwości mechanicznych dwóch kompozytów na osnowie stopu magnezu QE22. Kompozyt umacniany 20% obj. krótkich włókien Al_2O_3 oraz kompozyt hybrydowy umacniany 5% obj. włókien Al_2O_3 i 15% obj. cząstek SiC odkształcano poprzez ściskanie od temperatury pokojowej (RT) do 400°C. Dodatkowo, w celach porównawczych, badaniom poddano również sam stop osnowy QE22. Wyznaczono charakterystki naprężeń σ_{02} oraz σ_{mx} w zależności od temperatury. Badaniom poddano dwa rodzaje próbek: z włóknami ukierunkowanymi równolegle i prostopadle do osi naprężeń. Badania mikrostrukturalne materiałów kompozytowych przeprowadzono z zastosowaniem mikroskopii optycznej oraz skaningowej mikroskopii elektronowej. Poddano dyskusji możliwe mechanizmy umacniania i uplastyczniania badanych materiałów.

Słowa kluczowe: **kompozyty, kompozyty hybrydowe, umacnianie, uplastycznianie**

INTRODUCTION

The commercial QE22 alloy was derived from Mg-Re-Zr alloys by the addition of silver, which improves the mechanical properties of alloy. The QE22 alloy displays good creep resistance that is attributed to both the strengthening effect of precipitates and the presence of the grain boundary phases which reduce the grain boundary sliding. Ageing causes precipitation within the grains. The precipitation process depends on silver content [1]. If the silver content is less than 2 wt.%, the precipitation process appears to be similar to that occurring in Mg alloys with rare earths (mainly Nd), i.e. starts with the GP zones (Mg-Nd, coherent platelets paralell with $\{10\bar{1}0\}_{Mg}$ planes) and finishes with $Mg_{12}Nd$ incoherent precipitates. For higher amounts of silver two independent precipitation processes have been reported both started with GP zones, rodlike or ellipsoidal, respectively, and leading ultimately to the formation of an equilibrium phase of probable composition $Mg_{12}Nd_2Ag$ [2]. Considerable improvement of the mechanical properties as well as the thermal stability can be achieved by the reinforcement by ceramic fibres. Magnesium matrix composites show better wear resistance, enhanced strength and creep resistance and keep low density and good machinability [3-5]. Benefits of the fibre reinforcement can be powered by precipitation hardening in the matrix.

The objectives of the present paper are to study the deformation behaviour of the QE22 alloy based composites and to discuss possible contribution of Saffil ceramic fibres and SiC particles to the strengthening as well as the softening of these materials.

EXPERIMENTAL PROCEDURE

QE22 alloy (Mg - 2.5 wt.% Ag - 2 wt.% RE, mainly Nd - 0.6 wt.% Zr) was used as the matrix alloy. Composites with 20 vol.% short fibres of δ-Al_2O_3 (Saffil®) and hybrid composites with 5 vol.% of Saffil short fibres and 15 vol.% of SiC particles were prepared by squeeze casting technique. The performs consisted of planar randomly distributed Saffil fibres as well as

[1] RNDr., PhD, [2] Prof. RNDr., DrSc, [3] Mgr.

Saffil fibres with equiaxial SiC particles. Microstructure of the hybrid composite is introduced in Figure 1. Saffil fibres as well as SiC particles are visible. Samples used in this study exhibited two orientations of the fibres plane - perpendicular and parallel to the specimen longitudinal axis (the stress axis).

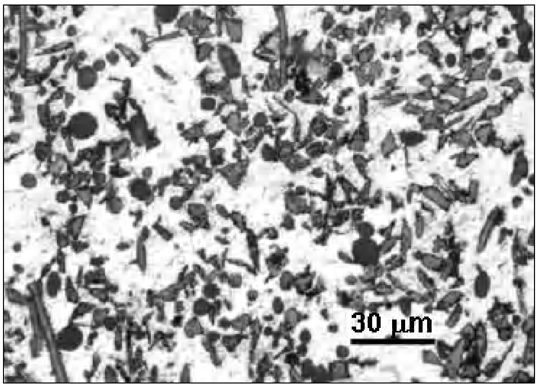

Fig. 1. Microstructure of QE22 hybrid composite (with Saffil fibres and SiC particles)

The mean fibre length and fibre diameter (measured after squeeze casting) were 78 and 3 µm respectively. The composites were subjected to a standard T6 heat treatment (anneal for 5.5 h at 520°C in the protective argon atmosphere, then age for 8 h at 205°C [2]). Samples for compression tests, machined from a composite block, exhibited the square cross-section of 5 x 5 mm and the length of 10 mm. Samples were deformed in an Instron 1186 testing machine at an initial strain rate of 8.3 x 10^{-5} s^{-1} in the temperature interval from room temperature up to 400°C. Temperature in the furnace was kept with an accuracy of ±1°C. Experiments at elevated temperatures were performed in a protective argon atmosphere. Metallographic and SEM inspection was performed with the aim to document microstructure and fracture surfaces of composites.

EXPERIMENTAL RESULTS

Stress-strain curves for unreinforced QE22 alloy deformed at various temperatures are introduced in Figure 2. Specimens were tested to the final fracture, at elevated temperatures the tests were interrupted at the strain of approximately 30%. From Figure 2 it can be seen that deformation stresses decrease with increasing temperature. The temperature dependencies both the yield stress σ_{02} as well as the maximum stress σ_{max} for QE22 alloy are shown in Figure 3. Both the yield and the maximum stresses decrease with increasing temperature for temperatures higher than 100°C. The maximum stresses decrease rapidly for temperatures above 200°C. The difference between both stresses is very small for temperatures 350 and 400°C.

Figure 4 shows the stress-strain curves obtained for QE22/Al_2O_3 composite deformed at various temperatures. Presence of the reinforcement leads to substantial decrease of the overall ductility. Samples at all temperatures were deformed to fracture excepting curve obtained at 400°C, where the compression test was interrupted.

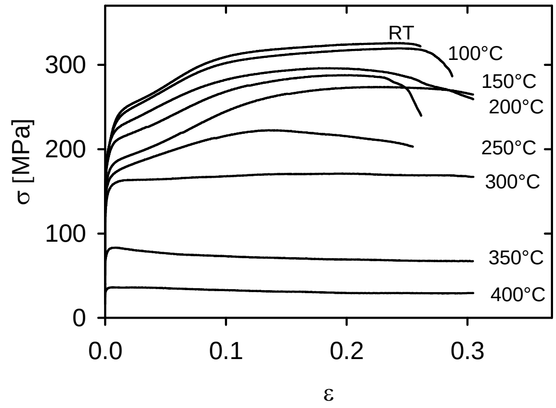

Fig. 2. True stress-true strain curves obtained for the QE22 matrix alloy

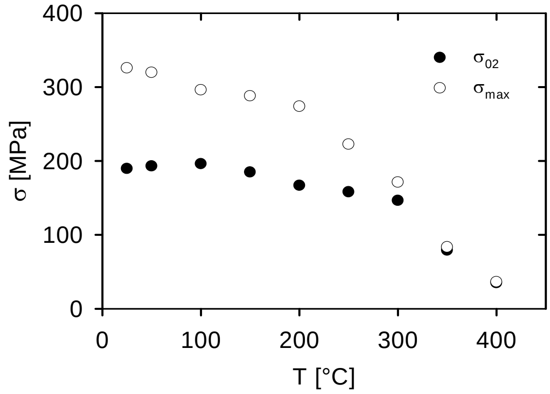

Fig. 3. Temperature dependencies of the characteristic stresses for QE22 unreinforced matrix

Temperature dependencies of the characteristic stresses σ_{02} and σ_{max} for the composite QE22+20 vol.% Al_2O_3 with the fibres plane parallel to the stress axis (||) are introduced in Figure 6. For temperatures up to 150°C the characteristic stresses are higher in comparison with unreinforced alloy. Both the yield and the maximum stresses decrease with increasing temperature very rapidly for temperatures higher then 300°C and the reinforcing effect of fibres is weak in this high temperature interval. The stress-strain curves obtained at various test temperatures and the temperature dependencies of characteristic stresses for QE22 composite with the fibres plane perpendicular to the stress axis (⊥) are introduced in Figures 6 and 7. Pronounced difference in comparison with the previous two figures can be seen. Characteristic stresses achieved for ⊥ fibres plane orientation are significantly lower in comparison with the sample exhibited parallel fibres plane (||). On the other hand, the ductility of ⊥ samples is substantially higher, especially at higher temperatures, comparable with the unreinforced alloy. Compression tests were interrupted at temperatures 200÷400°C. Marked softening was observed at temperature of 400°C.

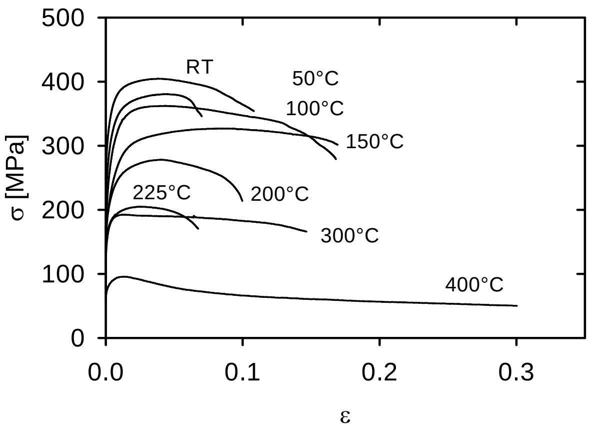

Fig. 4. True stress-true strain curves for $QE22/Al_2O_3$ in || orientation obtained at various temperatures

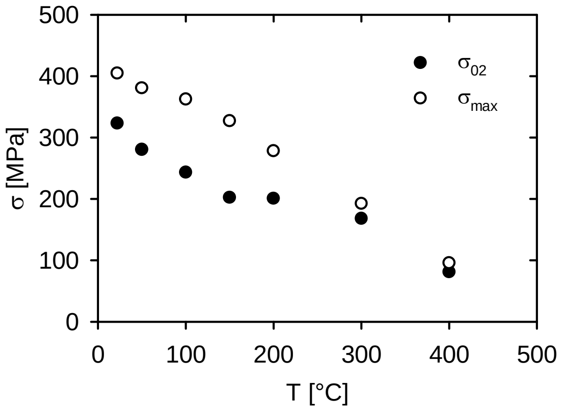

Fig. 5. Temperature dependencies of the characteristic stresses for $QE22/Al_2O_3$ in || orientation

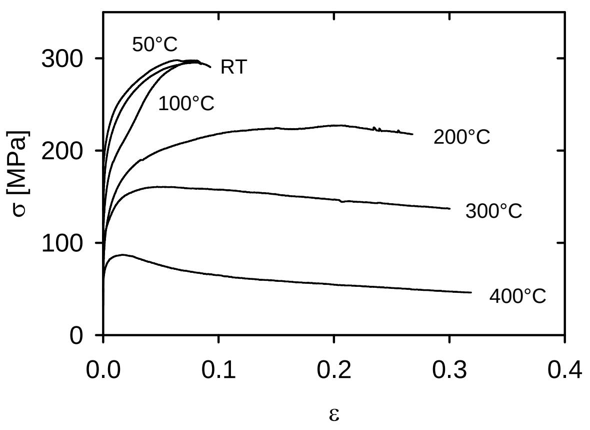

Fig. 6. True stress-true strain curves for $QE22/Al_2O_3$ in ⊥ orientation obtained at various temperatures

Characteristic stresses σ_{02} and σ_{max} decrease with increasing temperature excepting temperature of 50°C. Such small local maximum in the temperature dependence of the yield stress was observed also in other magnesium alloys (AZ91, LA45) [6, 7]. The difference between both orientations ⊥ and || is at 400°C very small. From Figures 3 and 7 it can be seen that mechanical properties of the unreinforced QE22 alloy are comparable with the perpendicular oriented (⊥) composite.

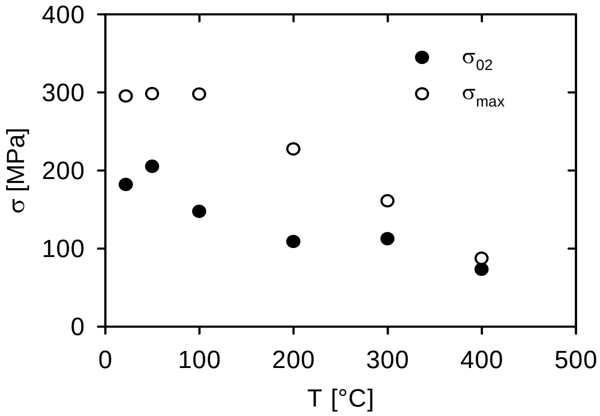

Fig. 7. Temperature dependencies of the characteristic stresses for $QE22/Al_2O_3$ in ⊥ orientation

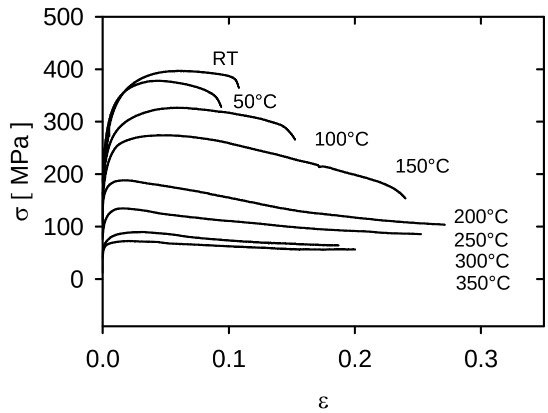

Fig. 8. True stress-true strain curves for QE22 with Saffil fibres and SiC particles in || orientation obtained at various temperatures

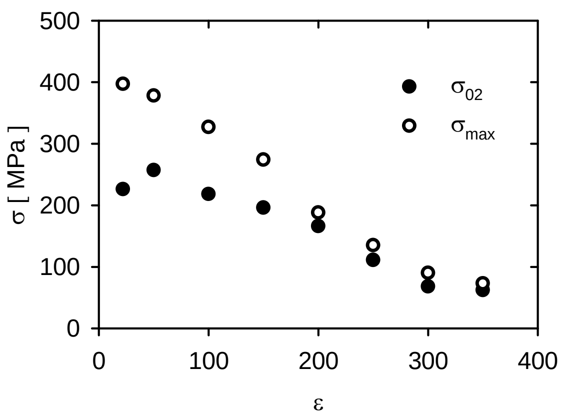

Fig. 9. Temperature dependencies of the characteristic stresses for QE22 with Saffil fibres and SiC particles in || orientation

Similar experiments were performed for hybrid composites (QE22 with Saffil fibres and SiC particles) with two orientations of the fibres plane. The stress--strain curves and the temperature dependencies of the characteristic stresses for QE22 hybrid composite are introduced in Figures 8 and 9 (|| orientation of the fibres plane) and Figures 10, 11 for perpendicular orientation of the fibres plane (⊥ orientation).

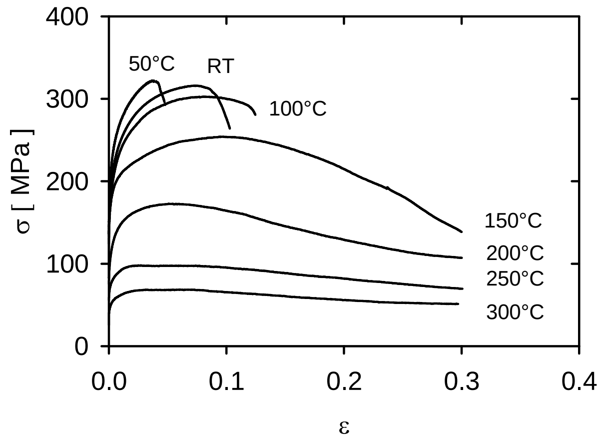

Fig. 10. True stress-true strain curves for QE22/Al_2O_3/SiC hybrid in ⊥ orientation obtained at various temperatures

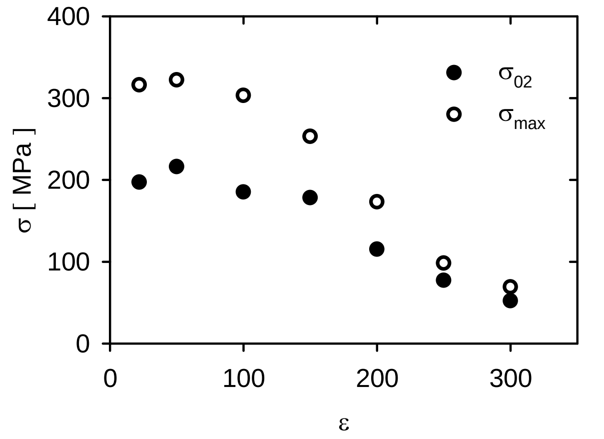

Fig. 11. Temperature dependencies of the characteristic stresses for QE22/Al_2O_3/SiC hybrid in ⊥ orientation

The influence of fibres in samples with the parallel oriented fibres plane is again well seen. The ductility is for hybrid || very good and higher then that obtained for composite || at elevated temperatures. There are no significant difference in characteristic stresses for hybrid and composite samples. The yield stress exhibits a local maximum at 50°C for hybrid || as well as for hybrid ⊥. This local maximum in the temperature dependence of the yield stress is very probably a consequence of the dynamic strain ageing phenomenon, where mobile solute atoms interact with dislocations. Both composite and hybrid exhibit lower ductility than monolithic QE22 alloy (matrix of investigated composite materials).

DISCUSSION

Influence of the reinforced phase

Composite materials are really inhomogeneous in both elastic as well as plastic properties. While the reinforcing phase remains usually due to mechanical loading of composite only elastic deformed, plastic deformation goes on in the matrix. In our previous papers [8, 9] we discussed various hardening mechanisms in Mg-Li-Al alloys reinforced by 10% of short Saffil fibres. The most important contributions were found load transfer on fibres and influence of the increased dislocation density arising from internal thermal stresses. Other possible mechanisms are minority and they do not influence the level of deformation stresses by significant manner.

The load transfer from matrix to fibres can be described by the shear lag theory [10] which assumes that the load transfer occurs between a high aspect ratio reinforcement and the matrix by means of shear stress at the interface between fibres and matrix. A contribution to the yield stress is than done by following equation:

$$\Delta\sigma_{LT} = \sigma_m\left[\frac{(L+t)A}{4L}\right]f + \sigma_m(1-f) \qquad (1)$$

where $\Delta\sigma_{LT}$ is the contribution to the yield stress, σ_m is the yield stress in the matrix, L is the fibre size in the stress direction, t is the fibre size in the perpendicular direction, A is equal to L/t, f is the volume fraction of reinforcing fibres in matrix. From the equation (1) it follows that possible influence of particles may be weaker due to low value of the aspect ratio A.

Typical big difference between coefficient of thermal expansion (CTE) of the matrix and ceramic reinforcement is very important factor in composites with a metallic matrix. CTE of a ceramic reinforcement is smaller than that of most metallic matrices. When the metal matrix composite is cooled from a higher temperature to room temperature, misfit strains occur because of differential thermal contraction at the interface. These strains induce thermal stresses that may be higher than the yield stress of the matrix. Thermal stresses may be sufficient to generate new dislocations at the interfaces between the matrix and the reinforcements. Therefore, after cooling the composite, the dislocation density in the matrix increases. The increase in the dislocation density near reinforcement fibres has been calculated as [11]

$$\Delta\rho = \frac{Bf\Delta\alpha\Delta T}{b(1-f)}\,\frac{1}{t} \qquad (2)$$

where f is the volume fraction of the reinforcement, t is its minimum size, b is the magnitude of the Burgers vector of the newly created dislocations, B is a geometrical constant. When the thermal stresses achieves the yield stress, plastic zones can be formed in the matrix near to the interfaces, especially, in the vicinity of fibre ends. We believe that the higher dislocation density arises in composites during the fabrication procedure. The generation of thermally induced dislo-cations and the related dislocations density gradients increase also the yield stress of the composite according to the well-known relationship

$$\Delta\sigma_{CTE} = \alpha_1 \psi G b (\Delta\rho)^{1/2} \quad (3)$$

where α_1 is a constant, ψ is the Taylor factor and G is the shear modulus. This high matrix dislocation density as well as the reinforcement/matrix interfaces can provide high diffusivity path in a composite. The higher dislocation density would also affect the precipitation kinetics in a precipitation hardenable matrix.

Microstructural changes in the matrix

Discontinuously reinforced composites usually have very fine grains, smaller than their unreinforced matrices. The contribution to the yield stress can then be estimated using the Hall-Petch relation, which relates the yield stress enhancement to grain size d

$$\Delta\sigma_{GS} = K \mathrm{d}^{-1/2} \quad (4)$$

where K is a constant. Metallographic investigation of QE22/Al_2O_3 composites revealed really smaller grain size in composite. This is demonstrated in Figures 12 and 13, where grains in QE22 monolithic alloy as well as in composite are visible.

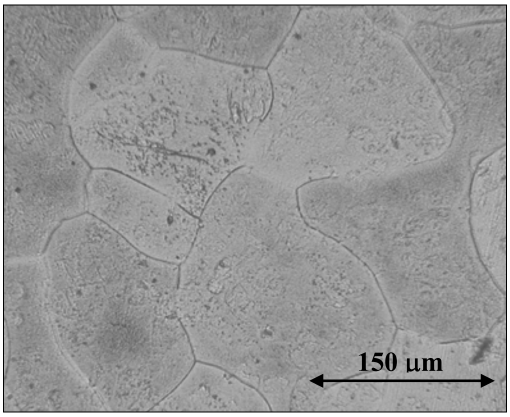

Fig. 12. Microstructure of QE22 monolithic alloy after T6 heat treatment. Grain boundaries and small precipitates are are visible

Kiehn et al. [12] have estimated that ceramic fibres and the reaction products of the inorganic binder (containing Al_2O_3) in the preform enhanced the Al concentration due to decomposition in the QE22 matrix. Contrary to the unreinforcement alloy Ag remains dissolved in the matrix of the reinforced alloy and does not take part in the precipitation process. Then matrix in the composite contains different precipitates than the monolithic alloy. Svoboda et al. [13], who studied the microstructure of QE22 alloy with SiC particulates after T6 thermal treatment, have reported two types of Mg_3(Ag,Nd) precipitates, rod-like precipitates of complex chemical composition including Zr and Nd and tiny MgO particles were observed as main secondary phases. Such precipitation detrimentally affect strength of the matrix.

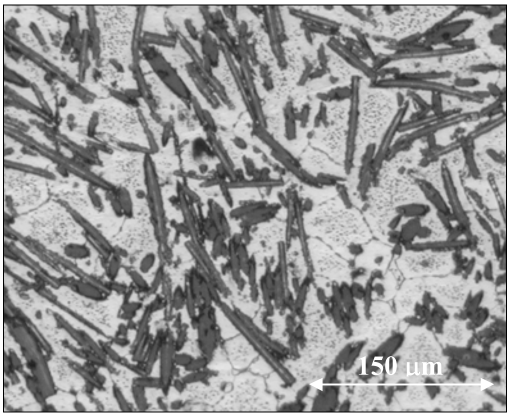

Fig. 13. Saffile fibres in the QE22 matrix. Grain size is smaller in comparison with the matrix alloy

Softening processes

Observed forms of stress strain curves at elevated temperatures, where maximum stress was achieved already at lower strain and subsequent stress decrease indicate an operating of recovery mechanisms. Cross slip in prismatic or pyramidal planes is very probably the main recovery mechanism. These mechanisms are strongly thermally activated. Increased activity of non-basal slip systems with <c+a> dislocations at higher temperatures provides explanation for observed decrease of the flow stress. The cross slip as well as the subsequent annihilation of dislocations results in a decrease in the work hardening rate.

Plastic deformation in a composite begins by developing of the strain in the vicinity of fibres, where dislocation density is higher than elsewhere in the matrix. Dislocations cannot pass through the fibers without cutting them or leaving loops around fibers. This passing mechanism is similar to the Orowan mechanism and it is also athermal. Dislocations pile-ups behind of fibres can act as stress concentrators. Screw dislocation components locally cross slip, forming superjogs having a height of about fibre diameter and at higher temperatures edge components are able to climb. Both may then annihilate in neighbouring slip planes. Possible annihilation of dislocations may be also support by interfacial diffusion of vacancies in the thin layer at the matrix-fibre interface [14].

Influence of interface

In composites the role of the interface is crucial. Stiffening and strengthening rely on load transfer across the interface. Interfacial stresses can arise from differential thermal contraction and from prior plastic flow of the matrix, as well as by the application of an external load. Weakening of interfaces at elevated temperatures can have large effect on composites deformation behaviour. The fracture surface of the hybrid composite, deformed at room temperature is introduced in Figure 14. By contrast the intensive debonding of the matrix/fiber interface was revealed at the fracture interfaces of composites deformed at elevated temperatures (Fig. 15).

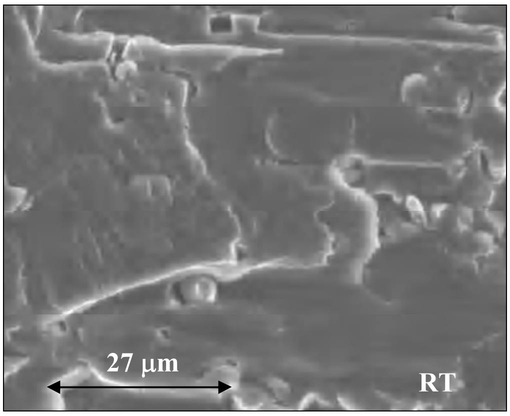

Fig. 14. Fracture surface of hybrid ⊥ deformed at RT

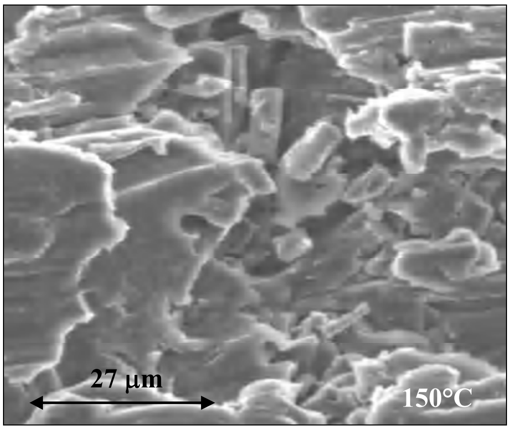

Fig. 15. Fracture surface of hybrid ⊥ deformed at 150°C. Debonding of fibers is visible

CONCLUSIONS

1. Ceramics fibres and particles influence significantly mechanical properties of composites with the QE22 matrix.
2. Short fibres contribute better to strengthening of the composite.
3. Perpendicular orientation of the fibres plane has weaker influence on the composite deformation properties.
4. Paralell orientation of the fibres plane in composites markedly increased characteristic stresses. This fibres impact decreases with increasing temperature.
5. Main hardening mechanism in composite is probably the load transfer in which the part of the external load within the matrix is transferred to reinforcement. Increased dislocation density plays also important role.
6. The cross slip and subsequent annihilation of dislocations cause very probably softening in the matrix. Local climb of dislocations in the vicinity of fibres supported by interfacial diffusion is probably important recovery mechanism.
7. Different precipitates in the monolithic alloy and in the matrix of the composite and hybrid material contribute by different way to the precipitation hardening in the matrix.
8. Interfacial reaction zone around the reinforcement must be better understood.

Acknowledgements

This investigation was financially supported by the Grant Agency of the Academy of Sciences of the Czech Republic under grant A2041203.

REFERENCES

[1] Svoboda M., Pahutová M., Moll F., Březina J., Sklenička V., (In:) Magnesium Alloys and their Applications, ed. K.U. Kainer, Deutsche Gesellschaft fűr Materialkunde e. V., Wiley-VCH Weinheim 2000, 234-239.
[2] Polmear I.J., Mater. Sci. Technology 1994, 10, 1-16.
[3] Kainer K.U., Magnesium Alloys and their Applications, eds. B.L. Mordike, F. Hehmann, DGM, Oberursel 1992, 415.
[4] Oakley R., Cochrane R.F., Stevens R., Key Engn. Mater. 1995, 104/107, 387.
[5] Wilks T.E., King J.F., Magnesium Alloys and their Applications, eds. B.L. Mordike and F. Hehmann, DGM, Oberursel 1992, 431-437.
[6] Trojanová Z., Lukáč P., Gabor P., Drozd Z., Máthis K., Kovové Mater. 2001, 39, 368-378.
[7] Drozd Z., Trojanová Z., Gärtnerová V., Magnesium Alloys and their Applications, ed. K.U. Kainer, DGM, Willey 2003, 122.
[8] Kúdela S., Trojanová Z., Kolenčiak V., Lukáč P., Proc. of the Third International Conference 24-26 August 2000, Bangalore, India, Foundtion for Advanced Materials Education, Bangalore 2000, 679-686.
[9] Trojanová Z., Gärtnerová V., Lukáč P., Drozd Z., J. Alloys Comp. (in press).
[10] Aikin R.M. Jr., Christodoulou L., Scripta Metall. Mater. 1991, 25, 9.
[11] Arsenault J.R., Shi N., Mater. Sci. Engn. 1986, 81, 853.

[12] Kiehn J., Kainer K.U., Mordike B.L., Chmelík F., Lukáč P., Magnesium Alloys and their Applications, eds. B.L. Mordike, K.U. Kainer, Werkstoff-Informationsgesellschaft, Frankfurt 1998, 671.
[13] Svoboda A., Pahutová M., Moll F., Březina J., Sklenička V., (In:) K.U Kainer (ed.), Magnesium Alloys and their Applications, Wiley-VCH, Weinheim 2000, 234.
[14] Shewfelt R.S.W., Brown L.M., Phil. Mag. 1977, 35, 945.

Recenzent
Jerzy Sobczak